

Visual and Semantic Prompt Collaboration for Generalized Zero-Shot Learning

Huajie Jiang¹, Zhengxian Li¹, Xiaohan Yu², Yongli Hu^{1*}, Baocai Yin¹, Jian Yang², Yuankai Qi²

¹Beijing University of Technology ²Macquarie University

{jianghj, huyongli, ybc}@bjut.edu.cn, lisi@emails.bjut.edu.cn,

{xiaohan.yu, jian.yang, yuankai.qi}@mq.edu.au

Abstract

Generalized zero-shot learning aims to recognize both seen and unseen classes with the help of semantic information that is shared among different classes. It inevitably requires consistent visual-semantic alignment. Existing approaches fine-tune the visual backbone by seen-class data to obtain semantic-related visual features, which may cause overfitting on seen classes with a limited number of training images. This paper proposes a novel visual and semantic prompt collaboration framework, which utilizes prompt tuning techniques for efficient feature adaptation. Specifically, we design a visual prompt to integrate the visual information for discriminative feature learning and a semantic prompt to integrate the semantic formation for visual-semantic alignment. To achieve effective prompt information integration, we further design a weak prompt fusion mechanism for the shallow layers and a strong prompt fusion mechanism for the deep layers in the network. Through the collaboration of visual and semantic prompts, we can obtain discriminative semantic-related features for generalized zero-shot image recognition. Extensive experiments demonstrate that our framework consistently achieves favorable performance in both conventional zero-shot learning and generalized zero-shot learning benchmarks compared to other state-of-the-art methods.

1. Introduction

Generalized Zero-Shot Learning (GZSL) [42] aims to recognize images from both seen and unseen categories with the help of class semantic information, where class attributes [21, 26, 30, 62] and text descriptions [12, 32, 45] are widely used to transfer knowledge from seen classes to novel classes. GZSL is intrinsically inspired by the human cognitive ability to understand unknown concepts [30, 31, 42], gaining increasing attention recently.

Traditional approaches [1, 24, 38, 46, 55, 65] extract the

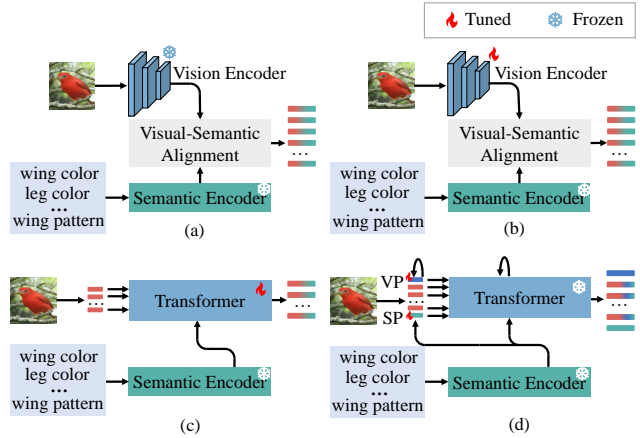


Figure 1. Different paradigms of GZSL. (a) Visual-semantic alignment with fixed backbone. (b) Fine-tuning visual features. (c) Fine-tuning with transformer backbone. (d) Our visual and semantic prompts collaboration network (VSPCN). The VSPCN integrates visual information and semantic information into the intermediate layers of the vision transformer network for semantic-related visual feature learning.

visual features and semantic features by pre-trained visual and language encoders independently and then align them in a common embedding space, as shown in Figure 1(a). However, visual features obtained via pre-trained models may not be well-aligned with the semantic features since they are independently extracted. To deal with this problem, some approaches [11, 62, 63, 69] propose to fine-tune the visual backbone to align with class semantics, as shown in Figure 1(b). Despite progress, the visual-semantic alignment is performed in the last layer of the network, which has less influence on the previous layers, resulting in less effective visual-semantic interaction. With the rapid development of the visual backbone network, transformer-based approaches have been proposed in zero-shot learning [7, 35, 67]. They perform visual-semantic interaction for different layers in the model, enabling more semantic-related features, as is shown in Figure 1(c). However, these approaches tend to overfit seen classes in the fine-tuning process due to limited

*Corresponding author

seen-class data.

To tackle this problem, we propose to utilize the prompt tuning technique to efficiently adapt the pre-trained model, and design a visual and semantic prompt collaboration network (VSPCN) for GZSL. Different from traditional prompt learning approaches, which only learn visual prompts, our VSPCN learns both visual and semantic prompts for better adaptive visual feature learning, as shown in Figure 1(d). The visual prompt aims to learn discriminative information by interacting with visual features, and the semantic prompt aims to learn class semantic information by interacting with the attributes. To further achieve effective interaction of prompts, visual features, and attributes, we design two types of information fusion mechanisms: weak prompt fusion and strong prompt fusion, which are incorporated into the shallow and deep layers of our model. Through the collaboration of visual and semantic prompts, we can obtain more effective semantic-related visual features. Simple yet effective, our method achieves the best performance on three benchmark GZSL datasets.

To summarize, our main contributions are as follows:

- We propose a visual and semantic prompt collaboration network that facilitates discriminative and semantic-relevant visual feature learning for generalized zero-shot recognition.
- We design weak and strong prompt fusion modules tailored to different model layers, achieving effective information fusion among prompts, visual features, and semantic features.
- Our method achieves the best performance on three GZSL benchmark datasets compared to other state-of-the-art approaches, demonstrating its effectiveness.

2. Related Work

Generalized Zero-Shot Learning. Semantic information plays an important role in GZSL. Based on the approach of utilizing semantic information, current GZSL methods can be roughly divided into two categories: generative-based GZSL methods and embedding-based GZSL methods.

Generative-based GZSL approaches aim to generate image features for the unseen classes using different generative models, such as generative adversarial nets (GANs) [4, 17, 20, 23, 24, 28, 33, 58, 61], variational autoencoders (VAEs) [16, 39, 48, 50, 66], and denoising diffusion models [13, 15, 40]. Then they train GZSL classifiers using both the real seen-class visual features and the synthesized unseen-class visual features for recognition. Although these approaches have achieved great progress, the generative models may be difficult to train. Moreover, the feature-generation process is independent of the recognition process, which makes the generated features less effective for recognition.

The embedding-based GZSL methods aim to align visual space and semantic space through visual-semantic mapping and perform image recognition in a common semantic space. Earlier embedding-based works [25, 27, 47, 59, 65] directly project the global visual features into the sharing space for category predictions. However, the global visual features fail to capture local discriminative representations, leading to sub-optimal classification performance. Therefore, the attention-based approaches [5, 6, 62, 63], have been adopted to highlight discriminative visual features related to attributes. Recent works [7, 35, 53, 68] deploy the semantic-visual attention module to progressively update semantic attributes and visual features together, which improves the consistency of visual features and semantic features. Though great progress has been made, these works fine-tune the backbone with limited numbers of seen-class data, improving the risk of overfitting the seen classes.

Different from existing approaches, which fine-tune the backbone to obtain semantic-relevant visual features, we adopt an effective prompt learning mechanism to adapt the pre-trained model to the GZSL task.

Prompt Learning for Vision Transformer. Prompt learning bridges the gap between pre-training models and downstream tasks, enabling effective adaptation to the downstream tasks. Vision transformers utilizing prompt engineering demonstrate remarkable performances in various visual tasks, such as compositional zero-shot learning [37, 41, 54], few-shot learning [10], and continuous learning [56, 57]. DFSP [37] and CSP [41] introduce soft prompt, a parameter-efficient learning technique that tunes a subset of tokens within the vocabulary to represent primitive concepts. SP [10] proposes a novel semantic prompt approach to leveraging textual information in class names for few-shot image recognition, which aims to adaptively adjust pre-trained visual features to class-specific features. L2P [57] and Dual-prompt [56] utilize prompt learning to learn new classes and simultaneously keep the knowledge of old classes.

Different from the above prompt learning approaches, we propose a novel visual and semantic prompt collaboration framework, which simultaneously learns visual and semantic prompts for effective semantic-related visual feature learning. Moreover, we design weak and strong prompt fusion methods tailored to different ViT layers, achieving effective information fusion among prompts, visual features, and semantic features.

3. Method

Problem Formalization. Zero-Shot learning aims to transfer knowledge from seen class \mathcal{D}^s , to unseen classes \mathcal{D}^u in the inference. $\mathcal{D}^s = \{(x^s, y^s, a_y^s) | x \in \mathcal{X}^s, y \in \mathcal{Y}^s, a_y^s \in \mathcal{A}^s\}$, where x^s refers to the image in \mathcal{X}^s , y^s refers to the corresponding label and a_y^s refers to the corresponding category semantic attributes from seen class datasets. Similarly,

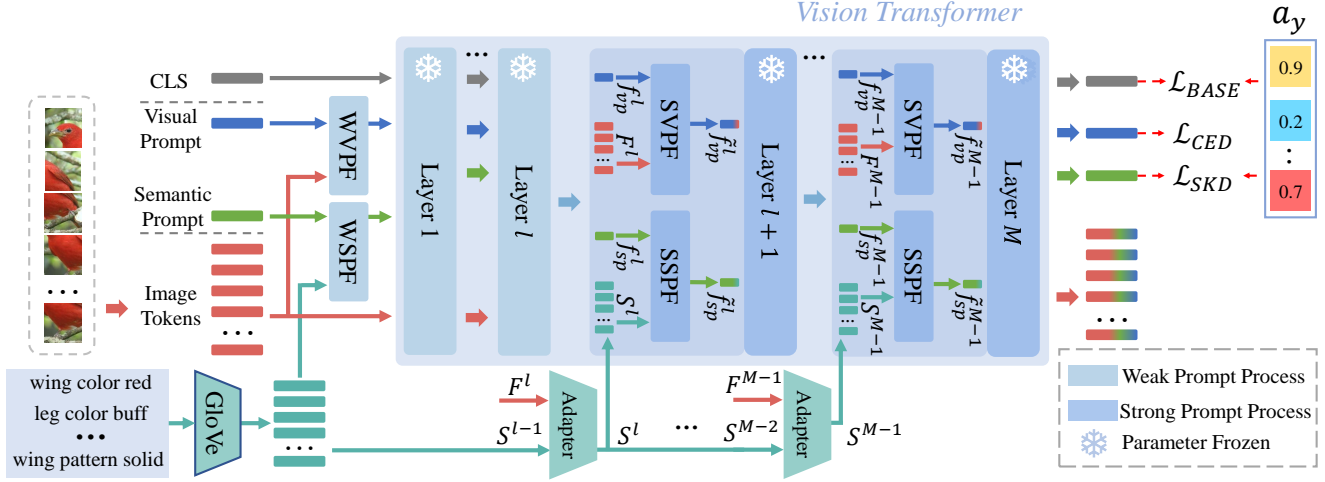


Figure 2. The framework of visual semantic prompts collaboration network (VSPCN). VSPCN utilizes the collaboration of visual and semantic prompts to adapt the pre-trained ViT model to the GZSL task. The visual prompt learns to extract visual information from image tokens, and the semantic prompt incorporates semantic information from semantic attributes. Weak prompt fusion (including weak visual prompt fusion (WVPF) and weak semantic prompt fusion (WSPF)) (3.1) and strong prompt fusion (including strong visual prompt fusion (SVPF) and strong semantic prompt fusion (SSPF)) (3.2) mechanisms are designed to integrate visual and semantic information. Furthermore, the adapters are utilized to update the semantic features for instance-level adaptive semantic information extraction (3.3).

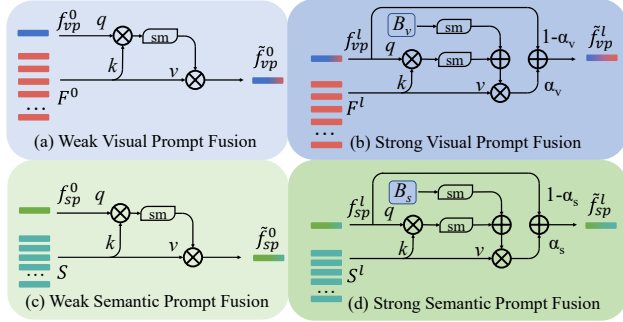


Figure 3. Illustration of our fusion modules. (a) weak visual prompt fusion, (b) strong visual prompt fusion, (c) weak semantic prompt fusion, and (d) strong semantic prompt fusion.

$\mathcal{D}^u = \{(x^u, y^u, a_y^u) | x \in \mathcal{X}^u, y \in \mathcal{Y}^u, a_y^u \in \mathcal{A}^u\}$, where x^u refers to an image in \mathcal{X}^u , y^u refers to the corresponding label and a_y^u refers to the corresponding category semantic attributes from unseen class datasets. Based on ZSL setting $\mathcal{Y}^s \cap \mathcal{Y}^u = \emptyset$, ZSL aims to learn a classifier for unseen classes $f_{zsl} : \mathcal{X} \rightarrow \mathcal{Y}^u$ predict the class labels \mathcal{Y} from the unseen set \mathcal{Y}^u , while GZSL aims to predict the class labels $\mathcal{Y} = \mathcal{Y}^s \cup \mathcal{Y}^u$ from both seen and unseen classes. In this paper, we use $S \in \mathbb{R}^{N_a \times D}$ to represent the sharing semantic attribute to describe the word vectors of attributes, which is abstracted by a language model **Glove** [44]. Among them, N_a and D represent the number of attributes and D represents the dimension of the Glove feature.

Overview. In order to extract semantic-related features effectively, we propose a visual and semantic prompt collaboration Network (VSPCN), which utilizes the prompt learning

mechanism to adapt the pre-trained model to specific GZSL tasks. Figure 2 provides an overview of the proposed method, where the pre-trained Vision Transformer (ViT) serves as the backbone network. VSPCN expects five inputs: CLS token, visual prompt, semantic prompt, image tokens, and shared semantic attributes. Among them, the CLS token, visual prompt, and semantic prompt are randomly initialized, image features are mapped from image patches, and shared semantic attributes are obtained from **Glove** [44]. To ensure effective information fusion among prompts, image features, and attributes, we design weak prompt fusion in the shallow layer (Section 3.1) and strong prompt fusion in the deeper layers (Section 3.2). Finally, we propose an entropy-based divergence loss for the visual prompt and a semantic knowledge distillation loss for the semantic prompt, ensuring discriminative and semantic feature learning (Section 3.3).

3.1. Weak Prompts Fusion

Weak prompt fusion aims to achieve information fusion in the early stage, which contains weak visual prompt fusion and weak semantic prompt fusion. As shown in Figure 3(a), the weak visual prompt aims at fusing the local visual features $F^0 = [f_1^0, f_2^0, \dots, f_{N_v}^0] \in \mathbb{R}^{N_v \times D}$ in each image token to extract visual prompt information, thereby enriching the randomly initialized visual prompt f_{vp}^0 . Specifically, we utilize the attention mechanism to achieve information fusion, which can be formulated as:

$$Q_v^0 = q(f_{vp}^0), K_v^0 = k(F^0), V_v^0 = v(F^0) \quad (1)$$

$$\tilde{f}_{vp}^0 = \delta \left(\frac{Q_v^0 K_v^{0T}}{\sqrt{D}} \right) V_v^0 \quad (2)$$

where \tilde{f}_{vp}^0 is a weak visual prompt updated by visual features, T denotes the transpose function, $q(\cdot)$, $k(\cdot)$ and $v(\cdot)$ are the linear mapping functions for the query, the key and the value. The $\delta(\cdot)$ is *softmax*() operation. Similarly, in order to enhance the semantic prompts, we fuse semantic information from shared semantic attributes by semantic attention, as shown in Fig 3(c):

$$Q_s^0 = q(f_{sp}^0), K_s^0 = k(S), V_s^0 = v(S) \quad (3)$$

$$\tilde{f}_{sp}^0 = \delta\left(\frac{Q_s^0 K_s^{0T}}{\sqrt{D}}\right) V_s^0 \quad (4)$$

where \tilde{f}_{sp}^0 is a weak semantic prompt updated by fine-grained attribute features. Compared to the original semantic prompt f_{sp}^0 , the weak semantic prompt \tilde{f}_{sp}^0 integrates semantic information and is closely linked to specific attribute features.

Weak prompt fusion is only conducted for the inputs. Then, we concatenate the CLS token, weak visual prompt, weak semantic prompt, and the image tokens to obtain $\tilde{F}^0 = [f_{cls}^0, \tilde{f}_{vp}^0, \tilde{f}_{sp}^0, f_1^0, f_2^0, \dots, f_{N_v}^0]$, which is utilized to perform feature learning in subsequent transformer layer. Afterward, the visual prompt, the semantic prompt, and visual features will interact in the ViT backbone by multi-head attention, achieving adaptive information fusion.

3.2. Strong Prompts Fusion

After calculating the first l layers of ViT, we can obtain the patch $F^l = [f_{cls}^l, f_{vp}^l, f_{sp}^l, f_1^l, f_2^l, \dots, f_{N_v}^l] = [f_{cls}^l, f_{vp}^l, f_{sp}^l, F^l]$. Since semantic information is only utilized for the inputs to enhance the semantic prompt, the semantic influence will be weakened in deeper layers, so we need to enrich the visual and semantic prompt information for the deeper layers. For this purpose, we design a strong prompt fusion mechanism for visual prompts and semantic prompts. As shown in Figure 3(b), we utilize an attention mechanism with bias estimation to learn the residual information to update the visual prompt f_{vp}^l . During the fusion process, the visual prompt is updated by image tokens and will not be affected by other tokens. When updating the visual prompt, the predicted attention bias $B_v^l \in \mathbb{R}^{N_v}$ are added to the attention matrix:

$$Q_v^l = q(f_{vp}^l), K_v^l = k(F^l), V_v^l = v(F^l) \quad (5)$$

$$\tilde{f}_{vp}^l = [\alpha_v \delta\left(\frac{Q_v^l K_v^{lT}}{\sqrt{D}}\right) + (1 - \alpha_v) \delta(B_v^l)] V_v^l + f_{vp}^l \quad (6)$$

where l indicates layer number, $\alpha_v \in (0, 1)$ represents the visual weight coefficient, F^l is the visual tokens output of the previous layer l . To enrich the semantic information of the semantic prompts, we further introduce the semantic information from shared semantic attributes to update the semantic prompt helping ViT extract semantic-related visual

features for zero-shot learning. As shown in Figure 3(d), this fusion process of the semantic prompt is achieved by a transformer with attention bias B_s^l . The formulation of semantic prompt in strong fusion is as follows:

$$Q_s^l = q(f_{sp}^l), K_s^l = k(S^l), V_s^l = v(S^l) \quad (7)$$

$$\tilde{f}_{sp}^l = [\alpha_s \delta\left(\frac{Q_s^l K_s^{lT}}{\sqrt{D}}\right) + (1 - \alpha_s) \delta(B_s^l)] V_s^l + f_{sp}^l \quad (8)$$

where S is sharing semantic attributes and is updated by the adapter under the influence of the image tokens, and $\alpha_s \in (0, 1)$ represents the semantic weight coefficient. Therefore, the prior knowledge from pre-trained NLP models is better transferred to the ViT features through the semantic prompt.

After obtaining the enhanced visual prompt \tilde{f}_{vp}^l and semantic prompt \tilde{f}_{sp}^l , we concatenate them with $[f_{cls}^l, f_1^l, f_2^l, \dots, f_{N_v}^l]$ to get $\tilde{F}^l = [f_{cls}^l, \tilde{f}_{vp}^l, \tilde{f}_{sp}^l, f_1^l, f_2^l, \dots, f_{N_v}^l]$, and then input \tilde{F}^l to lay $l+1$ for fine-grained feature extraction. Similarly, the subsequent ViT layers undergo the same strong prompt fusion process of visual and semantic prompts.

To enhance the semantic information for consistent information fusion, we design an adapter to learn adaptive semantic information for effective strong prompt fusion. Specifically, we interact the semantic information with the image features to learn instance adaptive semantic features using an attention mechanism, which can be formulated as:

$$Q_a^l = q(S^{l-1}), K_a^l = k(F^l), V_a^l = v(F^l) \quad (9)$$

$$S^l = \alpha_a \delta\left(\frac{Q_a^l K_a^{lT}}{\sqrt{D}}\right) V_a^l + (1 - \alpha_a) S^{l-1} \quad (10)$$

where $\alpha_a \in (0, 1)$ represents the hyperparameter.

3.3. Model Optimization and Inference

As shown in Fig.2, after completing the feature extraction of the ViT network, we obtain the final tokens $F^M = [f_{cls}^M, f_{vp}^M, f_{sp}^M, f_1^M, f_2^M, \dots, f_{N_v}^M]$. Then, we employ the base loss \mathcal{L}_{BASE} , the cross-entropy-based divergence loss \mathcal{L}_{CED} , and the semantic knowledge distillation loss \mathcal{L}_{SKD} to optimize our VSPCN.

Base Loss. As a major component, the base loss \mathcal{L}_{BASE} plays a role in image classification and semantic alignment and is composed of both the classification loss \mathcal{L}_{CLS} and the semantic regression loss \mathcal{L}_{AR} .

$$\mathcal{L}_{BASE} = \mathcal{L}_{CLS} + \gamma \mathcal{L}_{AR} \quad (11)$$

where γ is the weight parameter. For the classification loss, we first calculate the similarity between CLS token f_{cls}^M and the category semantic prototypes \tilde{a}_y , and then use the cross-entropy loss to calculate the classification loss:

$$\tilde{a}_y = a_y \cdot W_d \quad (12)$$

$$\mathcal{L}_{CLS} = -\log \frac{\exp(f_{cls}^M \cdot \tilde{a}_y^T)}{\sum_{\hat{y} \in \mathcal{Y}^s} \exp(f_{cls}^M \cdot \tilde{a}_{\hat{y}}^T)} \quad (13)$$

where W_d denotes the embedding parameter with the size of $N_a \times D$. At the same time, to promote alignment between CLS tokens and their corresponding real semantic prototypes, we introduced the semantic regression loss to optimize VSPCN by minimizing the mean square error:

$$\mathcal{L}_{AR} = \|f_{cls}^M - \tilde{a}_{gt}\|_2^2 \quad (14)$$

Cross-Entropy-Based Divergence Loss. In the process of ViT forward propagation, the visual prompt obtains prompt information from image tokens, so the visual prompt is similar to CLS tokens and can also be used for classification. However, to obtain divergence discriminative information different from CLS token, we propose a new regularization term, called the cross-entropy-based divergence loss \mathcal{L}_{CED} consisting of the cross-entropy loss \mathcal{L}_{CE} and the entropy-based divergence loss \mathcal{L}_{ED} .

$$\mathcal{L}_{CED} = \eta_1 \mathcal{L}_{CE}(\tilde{f}_{vp}^M \cdot W_c, y) + \eta_2 \mathcal{L}_{ED} \quad (15)$$

where η_1 and η_2 are the weights to control their corresponding loss terms, y is the corresponding label and W_c is the classifier with the size of $D \times N_s$ (N_s denotes the number of seen classes). Meanwhile, to ensure the visual prompt \tilde{f}_{vp}^M learns complementary information to the class token f_{cls}^M , we define the entropy-based divergence loss \mathcal{L}_{ED} :

$$\mathcal{L}_{ED} = \log\left(\frac{\mathcal{L}_{CE}(\tilde{f}_{vp}^M \cdot W_c, y) + \mathcal{L}_{CE}(f_{cls}^M \cdot W_c, y)}{\mathcal{L}_{KL}(\delta(\tilde{f}_{vp}^M), \delta(f_{cls}^M))} + 1\right) \quad (16)$$

where $\delta(\cdot)$ is a softmax function and \mathcal{L}_{KL} is the Kullback-Leibler divergence loss [29], which guides the vision prompt to gain discriminative knowledge itself while complementary to the knowledge from the CLS token.

Semantic Knowledge Distillation Loss. To learn effective semantic prompts, we propose a new semantic knowledge distillation loss \mathcal{L}_{SKD} . It is composed of a Jensen-Shannon Divergence (JSD) and an Euclidean distance, which enables the semantic prompt to align with its corresponding class semantic prototype. Given the semantic prompt \tilde{f}_{sp}^M and the semantic prototype a_y , semantic knowledge distillation loss \mathcal{L}_{SKD} is defined as:

$$\mathcal{L}_{SKD} = \frac{1}{2} \mathcal{L}_{KL}(\delta(f_s^M), \delta(\tilde{a}_y)) + \frac{1}{2} \mathcal{L}_{KL}(\delta(\tilde{a}_y), \delta(f_s^M)) + \|\tilde{a}_{gt} - f_s^M\|_2^2 \quad (17)$$

To this end, we formulate the overall loss function of VSPCN as follows:

$$\mathcal{L} = \mathcal{L}_{BASE} + \lambda_{CED} \mathcal{L}_{CED} + \lambda_{SKD} \mathcal{L}_{SKD} \quad (18)$$

where λ_{CED} and λ_{SKD} are the hyper-parameters to control the importance of each loss.

Inference. After training VSPCN, we first obtain the CLS token of test instance x through the ViT. Then, we apply an explicit calibration to adjust the predicted class probabilities and ensure balanced predictions across seen and unseen classes, which is formulated as follows:

$$\tilde{y} = \arg \max_{\hat{y} \in \mathcal{Y}^s \cup \mathcal{Y}^u} (f_{cls}^M \cdot a_{\hat{y}}^T + \tau \mathbb{I}_{\hat{y} \in \mathcal{Y}^u}) \quad (19)$$

where τ is a hyper-parameter to control the strength of the calibration applied to predictions for unseen classes, helping balance prediction biases between seen and unseen classes, and $\mathbb{I}_{\hat{y} \in \mathcal{Y}^u}$ is an indicator function which is zero when $\hat{y} \in \mathcal{Y}^s$.

4. Experiment

4.1. Experimental Settings

Benchmark Dataset. In order to demonstrate the effectiveness of the proposed visual and semantic collaboration framework, we follow ZSLViT to perform evaluation on three datasets Caltech-USCD Birds-200-2011 (CUB) [52], SUN Attribute (SUN) [43] and Animals with Attributes2 (AWA2) [60]. We follow the split setting according to Proposed Split (PS) [60] to split each dataset into seen and unseen classes.

Evaluation Protocols. During inference, we follow the evaluation protocol proposed by [60]. In the CZSL setting, we measure the accuracy of the test samples from the unseen classes (denoted Acc). In the GZSL setting, we compute the accuracy of the test samples from both seen classes (denoted S) and unseen classes (denoted as U). To generally evaluate the performance of VSPC in the GZSL setting, we use the harmonic mean (H), which balances the seen class accuracy S and the unseen class accuracy U . The harmonic mean is defined as $H = 2 \times S \times U / (S + U)$.

Implementation Details. Following the PSVMA [35], we adopt the ViT-Base [14] as the feature extractor, which is pre-trained on ImageNet-1k. We set the parameter $l=6$ and perform weak prompt fusion in the first 6 layers of vit, followed by strong prompt fusion in the following layers. We use the Adam optimizer with hyper-parameters (learning rate=0.001, weight decay=0.0001) to optimize our model. We implement our approach with PyTorch on NVIDIA RTX A4000.

4.2. Comparison with State-of-the-Arts

Conventional Zero-Shot Learning. Here, we first compare our VSPCN with the state-of-the-art methods in CZSL setting, where the performance is evaluated by the accuracy of the unseen classes in CZSL settings (Acc). As shown in Table 1, our VSPCN achieves the best accuracies of 80.6%,

	Methods	Backbone	CUB				SUN				AWA2			
			Acc	U	S	H	Acc	U	S	H	Acc	U	S	H
Generative	LsrGAN(ECCV'20) [51]	ResNet-101	60.3	48.1	59.1	53.0	62.5	44.8	37.7	40.9	66.4	54.6	74.6	63.0
	CE-GZSL (CVPR'21) [18]	ResNet-101	77.5	63.9	66.8	65.3	63.3	48.8	38.6	43.1	70.4	63.1	78.6	70.0
	FREE (ICCV'21) [8]	ResNet-101	-	55.7	59.9	57.7	-	47.4	37.2	41.7	-	60.4	75.4	67.1
	HSVA (NeurIPS'21) [9]	ResNet-101	62.8	52.7	58.3	55.3	63.8	48.6	39.0	43.3	-	56.7	79.8	66.3
	ICCE (CVPR'22) [28]	ResNet-101	78.4	67.3	65.5	66.4	-	-	-	-	72.7	65.3	82.3	72.8
	VS-Boost (IJCAI'23) [34]	ResNet-101	-	68.0	68.7	68.4	-	49.2	37.4	42.5	-	-	-	-
Embedding	DAZLE (CVPR'20) [22]	ResNet-101	66.0	56.7	59.6	58.1	59.4	52.3	24.3	33.2	67.9	60.3	75.7	67.1
	APN (NeurIPS'20) [63]	ResNet-101	72.0	65.3	69.3	67.2	61.6	41.9	34.0	37.6	68.4	56.5	78.0	65.5
	GEM-ZSL (CVPR'21) [36]	ResNet-101	77.8	64.8	77.1	70.4	62.8	38.1	35.7	36.9	67.2	64.8	77.5	70.6
	DPPN (NeurIPS'21) [53]	ResNet-101	-	70.2	77.1	73.5	-	47.9	35.8	41.0	-	63.1	86.8	73.1
	TransZero (AAAI'22) [5]	ResNet-101	76.8	69.3	68.3	68.8	65.6	52.6	33.4	40.8	70.1	61.3	82.3	70.2
	MSDN (CVPR'22) [6]	ResNet-101	76.1	68.7	67.5	68.1	65.8	52.2	34.2	41.3	70.1	62.0	74.5	67.7
	ICIS (ICCV'23) [12]	ResNet-101	60.6	45.8	73.7	56.5	51.8	45.2	25.6	32.7	64.6	35.6	93.3	51.6
	ZSCLR (ACM'24) [64]	ResNet-101	77.8	70.5	74.3	72.4	66.3	52.8	45.3	48.7	<u>76.0</u>	70.4	76.7	73.4
	ViT-ZSL (IMVIP'21) [3]	ViT-Large	-	67.3	75.2	71.0	-	44.5	55.3	49.3	-	51.9	90.0	68.5
	IEAM-ZSL (DGAM'21) [2]	ViT-Large	-	68.6	73.8	71.1	-	48.2	54.7	51.3	-	53.7	89.9	67.2
	DUET (AAAI'23) [11]	ViT-Base	72.3	62.9	72.8	67.5	64.4	45.7	45.8	45.8	69.9	63.7	84.7	72.7
	PSVMA (CVPR'23) [35]	ViT-Base	-	70.1	77.8	<u>73.8</u>	-	61.7	45.3	<u>52.3</u>	-	73.6	77.3	<u>75.4</u>
	ZSLViT (CVPR'24) [7]	ViT-Base	<u>78.9</u>	69.4	78.2	73.6	<u>68.3</u>	45.9	48.4	47.3	70.7	66.1	84.6	74.2
	VSPCN (Ours)	ViT-Base	80.6	72.8	78.9	75.7	75.3	59.4	49.1	53.8	76.6	71.8	84.3	77.6

Table 1. Results on CUB, SUN, and AWA2, including generative-based methods and embedding-based methods. ‘Acc’ denotes the accuracy of unseen classes in the setting of CZSL, ‘U’ denotes the accuracy of the unseen classes, ‘S’ denotes the accuracy of the seen classes, and ‘H’ is the harmonic mean in the setting of GZSL, which is the main measurement for GZSL. ‘H’ is the main metric for GZSL performance. ‘-’ denotes that the result is not reported. The best and second-best results are marked in bold and underline, respectively.

75.3%, and 76.6% on three datasets compared with previous methods, including both embedding-based methods and generative ZSL methods. These results demonstrate the effectiveness of VSPCN for CZSL. In the CZSL scenario, compared to the second best methods (e.g., ZSLViT [7] and ZSCLR [64]), our proposed method obtains gains over 1.7%, 7.0% and 0.6% on CUB, SUN, and Awa2, respectively. This indicates that VSPCN can effectively learn semantic-related visual features adapted by dual prompts collaboration, which enhances the transferability from seen classes to unseen classes.

Generalized Zero-Shot Learning. Table 1 also presents the GZSL results of different methods, including CNN features-based and ViT features-based methods. In the GZSL setting, our VSPCN achieves the best harmonic mean H of 75.7%, 53.8%, and 77.6% on CUB, SUN, and Awa2, respectively. Meanwhile, our VSPCN also outperforms the PSVMA [35] by 2.9%, 1.5%, and 2.2% on three datasets. In addition to harmonic mean H , we also perform well in the generalization of unseen classes, as can be seen by the U measurement. These benefits are achieved by the collaboration of visual and semantic prompts in VSPCN, which effectively adapt the pre-trained ViT model to the GZSL task, enabling semantic-related features that effectively generalize for knowledge transfer from seen to unseen classes. Noted that even compared with [2, 3] whose backbone is trained on ImageNet-21k, our model pre-trained on ImageNet-1k still achieves better performance.

4.3. Ablation Study

To give further insight into each component in our framework, we perform ablations to analyze the effectiveness of our VSPCN, as shown in Table 2. We conducted ablation experiments focusing on three key aspects: (1) visual and semantic prompts; (2) weak and strong fusion; (3) semantic adapter. We will discuss them in detail.

Effectiveness of visual and semantic prompts. In the VSPCN, we use the ViT as the baseline to extract visual features and calculate the similarity score with category prototypes. We also show the results of using visual and semantic prompts separately. Specifically, the model with visual prompt achieved a gain on H by (13.4%, 6.2%, 3.6%) on (CUB, SUN, AWA2) compared with the baseline, while the model with semantic prompt achieved a higher improvement by (14.6%, 7.0%, 11.2%). This indicates that the semantic prompt plays an important role in refining the semantic-related visual features. With the collaboration of visual and semantic prompts, the performance is improved.

Effectiveness of weak and strong fusion. We explore three situations: prompts without fusion, prompts with weak fusion, and prompts with strong fusion. The results in Table 2 (lines 3-6) indicate that both weak and strong fusions are necessary to achieve effective feature adaption.

Effectiveness of semantic adapter. We utilize adapters to adjust the semantic features. To demonstrate their effectiveness, we experiment without adapters, and the results are

baseline	Pv	Ps	WVPF	WSPF	SVPF	SSPF	CUB			SUN			AWA2		
							U	S	H	U	S	H	U	S	H
✓							63.3	55.9	59.3	67.6	34.0	45.2	54.9	79.9	65.0
✓	✓		✓		✓		68.7	77.2	72.7	60.3	44.8	51.4	60.5	79.2	68.6
✓		✓		✓		✓	70.1	78.0	73.9	59.2	46.7	52.2	71.4	81.7	76.2
✓	✓	✓					61.8	70.0	65.6	56.6	43.0	48.9	59.3	77.4	67.2
✓	✓	✓	✓	✓			73.5	70.0	71.7	61.9	45.6	52.5	70.1	75.1	72.5
✓	✓	✓			✓	✓	73.6	74.8	74.2	59.9	45.6	51.8	68.1	82.1	74.4
✓	✓	✓	✓	✓	✓	✓	72.5	77.4	74.9	60.8	46.9	52.9	65.7	80.1	72.2
✓	✓	✓	✓	✓	✓	✓	72.8	78.9	75.7	59.4	49.1	53.8	71.8	84.3	77.6

Table 2. Ablation studies of different components in VSPCN. 'Pv' is the visual prompt, and 'Ps' means the semantic prompt. 'WVPF', 'WSPF', 'SVPF', and 'SSPF' denote the weak visual prompt fusion, weak semantic prompt fusion, strong visual prompt fusion, and strong semantic prompt fusion, respectively. The ✓ indicates that the semantic attributes have been updated by adapters, while ✗ indicates no updation is conducted.

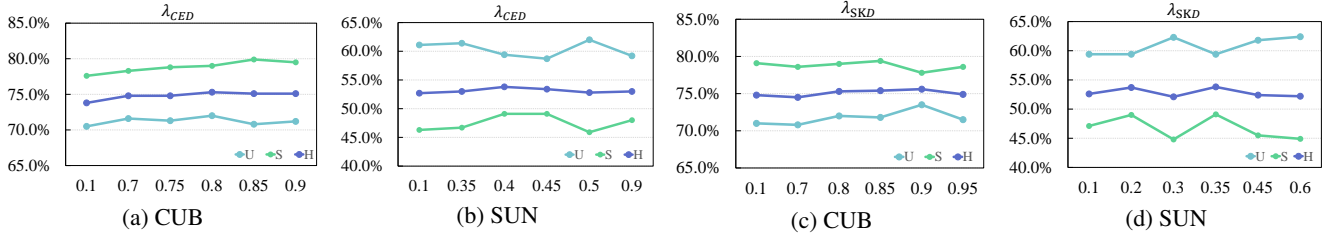


Figure 4. The effects of hyperparameters λ_{CED} and λ_{SKD} , which control the importance of visual and semantic prompts respectively.

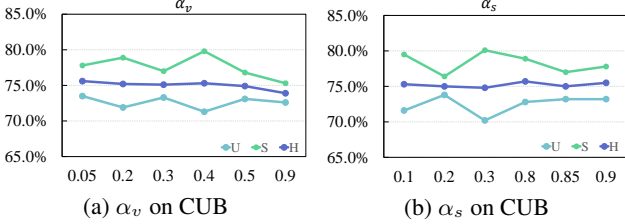


Figure 5. The impact of hyperparameters α_v and α_s to control the importance of self-attention and bias in the strong fusion process.

shown in the seventh line of Table 2. It can be seen that the performance drops without adapters, which indicates that it is necessary to learn adaptive semantic features.

4.4. HyperParameter Analysis

We perform experiments to investigate the effects of various hyper-parameters on CUB and SUN datasets, including λ_{CED} and λ_{SKD} in Eq. (18), α_v in Eq. (6) and α_s in the Eq. (8). From the results in Fig. 4 (a), with the increase of λ_{CED} , the harmonic mean raised slowly at first and then decreases when $\lambda_{CED} > 0.8$ on the CUB dataset. Larger λ_{CED} will enhance the visual prompt for discriminative feature learning. Similarly, as shown in Fig. 4 (b), VSPCN achieves better performances when the value is set as $\lambda_{CED} = 0.4$ on SUN. From Fig. 4 (c) and (d), it can be seen that as λ_{SKD} changes, U and S fluctuate significantly; hence, we choose $\lambda_{SKD}=0.9$ on CUB and $\lambda_{SKD}=0.35$ on SUN to obtain balanced performance between U and S .

The parameters α_v and α_s adjust the weight between the attention score and the bias score, which are utilized to fuse the prompt information. As shown in Fig.5 (a)(b), the optimal values for α_v and α_s are 0.05 and 0.8, which reflect that visual prompt focuses on attention score, while semantic prompt focuses on the bias scores on the CUB dataset.

4.5. Qualitative Results

Visualization of Visual Features. To gain an intuitive understanding of the visual features, we visualize the visual features extracted by our VSPCN using t-SNE [49]. As shown in Fig 6, we compare our approach with other approaches, including the CNN backbone (ResNet101 [19]), ViT-Base [14], and ZSLViT [7]. We choose 10 seen classes and 10 unseen classes for visualization, where 50 samples are randomly selected for each class. It can be seen that compared to ZSLViT and VSPCN, the features extracted directly using pre-trained CNN and ViT are less discriminative for different classes, so it is necessary to adapt the general model to specific tasks. Furthermore, comparing the results of ZSLViT and VSPCN, we can see that the visual features learned by VSPCN achieve better performance for intra-class compactness and inter-class separability, leading the classifier to learn appropriate classification boundaries.

Visualization of Attention maps. To intuitively demonstrate the effectiveness of our VSPCN framework, we visualized the attention maps of some samples on the CUB dataset. Specifically, we perform attention calculations on the CLS

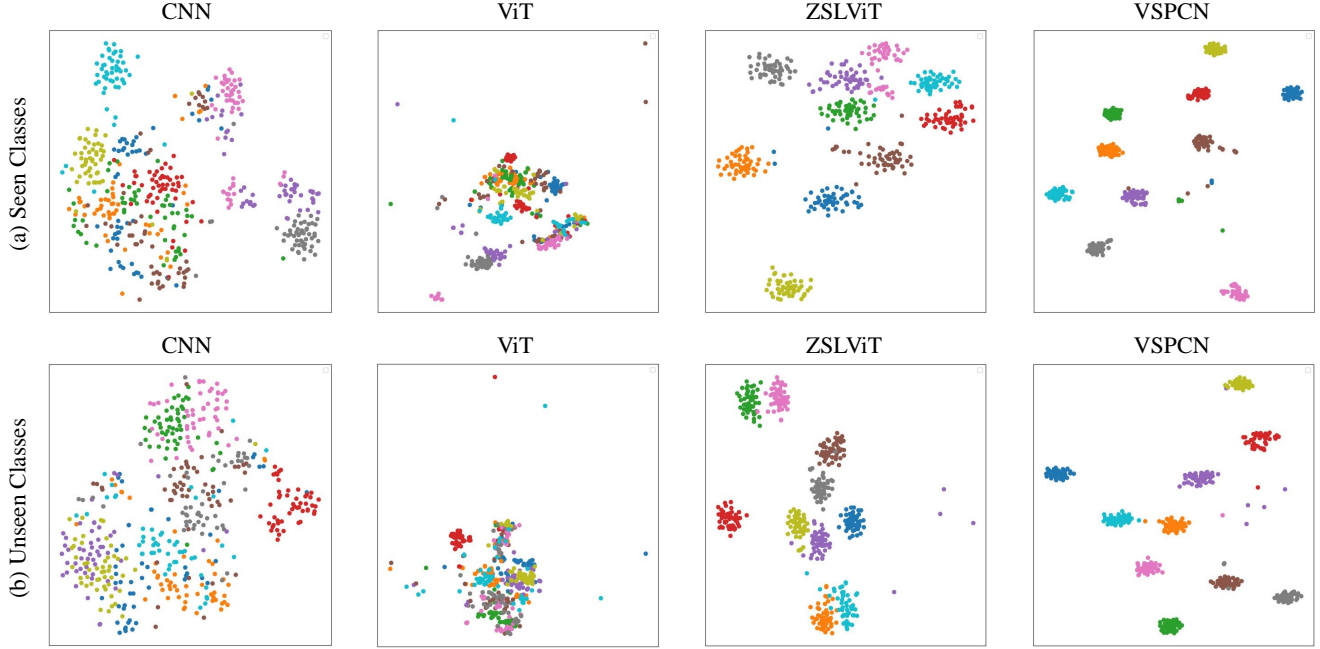


Figure 6. Feature visualization for seen classes and unseen classes on CUB by t-SNE. Different colors refer to different classes. We randomly select 10 classes and show the visualization results of different approaches.

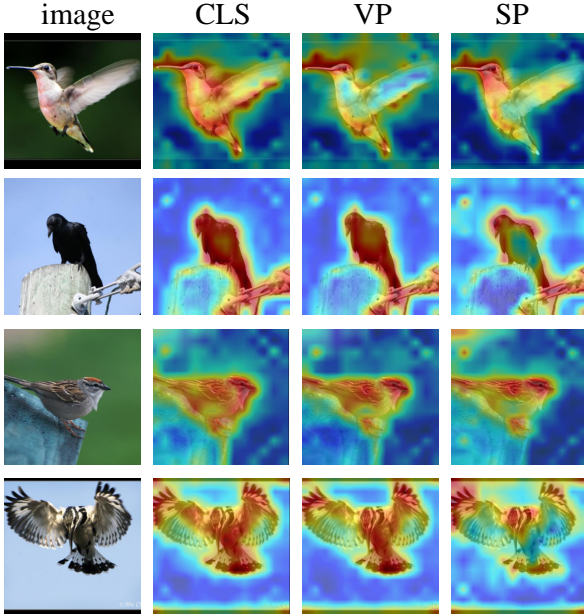


Figure 7. Visualization of attention maps obtained by CLS token, visual prompt (VP), and semantic prompt (SP), respectively.

token, visual prompt, and semantic prompt respectively, and the attention maps are shown in Fig. 7. We observe that both the visual prompt and semantic prompt are capable of identifying the key regions of objects. However, these regions represent only a portion of the object. In contrast, the CLS token (CLS) integrates information from both the visual prompt and the semantic prompt, which produces a more

comprehensive attention map. Therefore, we use the CLS token for recognition.

4.6. Conclusion

In this paper, we propose a Visual and Semantic Prompt Collaboration Network (VSPCN) for GZSL, where dual prompts complement each other to effectively adapt the pre-trained ViT model for semantic-relevant visual feature learning. Specifically, the visual prompt integrates the image features for discriminative information extraction and the semantic prompt integrates the semantic information for semantic information extraction. To achieve effective information integration, we further design weak and strong prompt fusion mechanisms for different layers in our model. Moreover, we design adapters to learn adaptive semantic features to enhance the semantic information. Through the collaboration of visual and semantic prompts, our framework can learn adaptive visual features that generalize well for novel categories. Extensive experiments on three benchmark GZSL datasets show the effectiveness of the proposed framework.

Acknowledgements. This work was supported by National Key R&D Program of China No.2021ZD0111902 and National Natural Science Foundation of China under Grant No.62206007 and Grant U21B2038. Xiaohan Yu, Jian Yang and Yuankai Qi are not supported by the aforementioned fundings.

References

- [1] Zeynep Akata, Florent Perronnin, Zaïd Harchaoui, and Cordelia Schmid. Label-embedding for attribute-based classification. In *CVPR*, pages 819–826, 2013. 1
- [2] Faisal Alamri and Anjan Dutta. Implicit and explicit attention for zero-shot learning. In *DAGM German Conference on Pattern Recognition*, volume 13024, pages 467–483, 2021. 6
- [3] Faisal Alamri and Anjan Dutta. Multi-head self-attention via vision transformer for zero-shot learning. *arXiv preprint arXiv:2108.00045*, 2021. 6
- [4] Dubing Chen, Yuming Shen, Haofeng Zhang, and Philip HS Torr. Deconstructed generation-based zero-shot model. In *AAAI*, pages 295–303, 2023. 2
- [5] Shiming Chen, Ziming Hong, Yang Liu, Guo-Sen Xie, Baigui Sun, Hao Li, Qinmu Peng, Ke Lu, and Xinge You. Transzero: Attribute-guided transformer for zero-shot learning. In *AAAI*, pages 330–338, 2022. 2, 6
- [6] Shiming Chen, Ziming Hong, Guo-Sen Xie, Wenhan Yang, Qinmu Peng, Kai Wang, Jian Zhao, and Xinge You. Msdn: Mutually semantic distillation network for zero-shot learning. In *CVPR*, pages 7612–7621, 2022. 2, 6
- [7] Shiming Chen, Wenjin Hou, Salman Khan, and Fahad Shahbaz Khan. Progressive semantic-guided vision transformer for zero-shot learning. In *CVPR*, pages 23964–23974, 2024. 1, 2, 6, 7
- [8] Shiming Chen, Wenjie Wang, Beihao Xia, Qinmu Peng, Xinge You, Feng Zheng, and Ling Shao. Free: Feature refinement for generalized zero-shot learning. In *ICCV*, pages 122–131, 2021. 6
- [9] Shiming Chen, Guosen Xie, Yang Liu, Qinmu Peng, Baigui Sun, Hao Li, Xinge You, and Ling Shao. Hsva: Hierarchical semantic-visual adaptation for zero-shot learning. In *NeurIPS*, pages 16622–16634, 2021. 6
- [10] Wentao Chen, Chenyang Si, Zhang Zhang, Liang Wang, Zilei Wang, and Tieniu Tan. Semantic prompt for few-shot image recognition. In *CVPR*, pages 23581–23591, 2023. 2
- [11] Zhuo Chen, Yufeng Huang, Jiaoyan Chen, Yuxia Geng, Wen Zhang, Yin Fang, Jeff Z Pan, and Huajun Chen. Duet: Cross-modal semantic grounding for contrastive zero-shot learning. In *AAAI*, pages 405–413, 2023. 1, 6
- [12] Anders Christensen, Massimiliano Mancini, A Koepke, Ole Winther, and Zeynep Akata. Image-free classifier injection for zero-shot classification. In *ICCV*, pages 19072–19081, 2023. 1, 6
- [13] Kevin Clark and Priyank Jaini. Text-to-image diffusion models are zero shot classifiers. *NeurIPS*, 2024. 2
- [14] Alexey Dosovitskiy, Lucas Beyer, Alexander Kolesnikov, Dirk Weissenborn, Xiaohua Zhai, Thomas Unterthiner, Mostafa Dehghani, Matthias Minderer, Georg Heigold, Sylvain Gelly, Jakob Uszkoreit, and Neil Houlsby. An image is worth 16x16 words: Transformers for image recognition at scale. In *ICLR*, 2020. 5, 7
- [15] Mengyu Gao and Qiulei Dong. Adaptive conditional denoising diffusion model with hybrid affinity regularizer for generalized zero-shot learning. *TCSVT*, 34:5641–5652, 2024. 2
- [16] Jiannan Ge, Hongtao Xie, Pandeng Li, Lingxi Xie, Shaobo Min, and Yongdong Zhang. Towards discriminative feature generation for generalized zero-shot learning. *TMM*, pages 1–16, 2024. 2
- [17] Akshita Gupta, Sanath Narayan, Salman Khan, Fahad Shahbaz Khan, Ling Shao, and Joost Van De Weijer. Generative multi-label zero-shot learning. *TPAMI*, 45:14611–14624, 2023. 2
- [18] Zongyan Han, Zhenyong Fu, Shuo Chen, and Jian Yang. Contrastive embedding for generalized zero-shot learning. In *CVPR*, pages 2371–2381, 2021. 6
- [19] Kaiming He, Xiangyu Zhang, Shaoqing Ren, and Jian Sun. Deep residual learning for image recognition. In *CVPR*, pages 770–778, 2016. 7
- [20] Wenjin Hou, Shiming Chen, Shuhuang Chen, Ziming Hong, Yan Wang, Xuetao Feng, Salman Khan, Fahad Shahbaz Khan, and Xinge You. Visual-augmented dynamic semantic prototype for generative zero-shot learning. In *CVPR*, pages 23627–23637, 2024. 2
- [21] Yongli Hu, Lincong Feng, Huajie Jiang, Mengting Liu, and Baocai Yin. Domain-aware prototype network for generalized zero-shot learning. *TCSVT*, 34:3180–3191, 2024. 1
- [22] Dat Huynh and Ehsan Elhamifar. Fine-grained generalized zero-shot learning via dense attribute-based attention. In *CVPR*, pages 4482–4492, 2020. 6
- [23] Huajie Jiang, Zhengxian Li, Yongli Hu, Baocai Yin, Jian Yang, Anton van den Hengel, Ming-Hsuan Yang, and Yuankai Qi. Dual prototype contrastive network for generalized zero-shot learning. *TCSVT*, 2024. 2
- [24] Huajie Jiang, Ruiping Wang, Shiguang Shan, and Xilin Chen. Learning class prototypes via structure alignment for zero-shot recognition. In *ECCV*, volume 11214, pages 121–138, 2018. 1, 2
- [25] Huajie Jiang, Ruiping Wang, Shiguang Shan, and Xilin Chen. Adaptive metric learning for zero-shot recognition. *IEEE Signal Processing Letters*, 26:1270–1274, 2019. 2
- [26] Huajie Jiang, Ruiping Wang, Shiguang Shan, and Xilin Chen. Transferable contrastive network for generalized zero-shot learning. In *ICCV*, pages 9764–9773, 2019. 1
- [27] Huajie Jiang, Ruiping Wang, Shiguang Shan, Yi Yang, and Xilin Chen. Learning discriminative latent attributes for zero-shot classification. In *ICCV*, pages 4233–4242, 2017. 2
- [28] Xia Kong, Zuodong Gao, Xiaofan Li, Ming Hong, Jun Liu, Chengjie Wang, Yuan Xie, and Yanyun Qu. En-compactness: Self-distillation embedding & contrastive generation for generalized zero-shot learning. In *CVPR*, pages 9296–9305, 2022. 2, 6
- [29] S. Kullback and R. A. Leibler. On information and sufficiency. *The Annals of Mathematical Statistics*, 22:79–86, 1951. 5
- [30] Christoph H. Lampert, Hannes Nickisch, and Stefan Harmeling. Learning to detect unseen object classes by between-class attribute transfer. In *CVPR*, pages 951–958, 2009. 1
- [31] Hugo Larochelle, Dumitru Erhan, and Yoshua Bengio. Zero-data learning of new tasks. In *AAAI*, volume 1, page 3, 2008. 1
- [32] Jimmy Lei Ba, Kevin Swersky, Sanja Fidler, and Ruslan salakhutdinov. Predicting deep zero-shot convolutional neural

- networks using textual descriptions. In *ICCV*, pages 4247–4255, 2015. [1](#)
- [33] Jingjing Li, Mengmeng Jing, Ke Lu, Zhengming Ding, Lei Zhu, and Zi Huang. Leveraging the invariant side of generative zero-shot learning. In *CVPR*, pages 7394–7403, 2019. [2](#)
- [34] Xiaofan Li, Yachao Zhang, Shiran Bian, Yanyun Qu, Yuan Xie, Zhongchao Shi, and Jianping Fan. Vs-boost: Boosting visual-semantic association for generalized zero-shot learning. In *IJCAI*, pages 1107–1115, 2023. [6](#)
- [35] Man Liu, Feng Li, Chunjie Zhang, Yunchao Wei, Huihui Bai, and Yao Zhao. Progressive semantic-visual mutual adaption for generalized zero-shot learning. In *CVPR*, pages 15337–15346, 2023. [1](#), [2](#), [5](#), [6](#)
- [36] Yang Liu, Lei Zhou, Xiao Bai, Yifei Huang, Lin Gu, Jun Zhou, and Tatsuya Harada. Goal-oriented gaze estimation for zero-shot learning. In *CVPR*, pages 3794–3803, 2021. [6](#)
- [37] Xiaocheng Lu, Song Guo, Ziming Liu, and Jingcai Guo. Decomposed soft prompt guided fusion enhancing for compositional zero-shot learning. In *CVPR*, pages 23560–23569, 2023. [2](#)
- [38] Pedro Morgado and Nuno Vasconcelos. Semantically consistent regularization for zero-shot recognition. In *CVPR*, pages 2037–2046, 2017. [1](#)
- [39] Sanath Narayan, Akshita Gupta, Fahad Shahbaz Khan, Cees GM Snoek, and Ling Shao. Latent embedding feedback and discriminative features for zero-shot classification. In *ECCV*, pages 479–495, 2020. [2](#)
- [40] Elvis Nava, Seijin Kobayashi, Yifei Yin, Robert K Katzschmann, and Benjamin F Grewe. Meta-learning via classifier (-free) diffusion guidance. 2023. [2](#)
- [41] Nihal V Nayak, Peilin Yu, and Stephen H Bach. Learning to compose soft prompts for compositional zero-shot learning. In *ICLR*. [2](#)
- [42] Mark Palatucci, Dean Pomerleau, Geoffrey E. Hinton, and Tom M. Mitchell. Zero-shot learning with semantic output codes. In *NeurIPS*, pages 1410–1418, 2009. [1](#)
- [43] Genevieve Patterson and James Hays. Sun attribute database: Discovering, annotating, and recognizing scene attributes. In *2012 IEEE Conference on Computer Vision and Pattern Recognition*, pages 2751–2758, 2012. [5](#)
- [44] Jeffrey Pennington, Richard Socher, and Christopher D Manning. Glove: Global vectors for word representation. In *empirical methods in natural language processing (EMNLP)*, pages 1532–1543, 2014. [3](#)
- [45] Scott Reed, Zeynep Akata, Honglak Lee, and Bernt Schiele. Learning deep representations of fine-grained visual descriptions. In *CVPR*, pages 49–58, 2016. [1](#)
- [46] Scott E. Reed, Zeynep Akata, Honglak Lee, and Bernt Schiele. Learning deep representations of fine-grained visual descriptions. In *CVPR*, pages 49–58, 2016. [1](#)
- [47] Jie Song, Chengchao Shen, Yezhou Yang, Yang Liu, and Mingli Song. Transductive unbiased embedding for zero-shot learning. In *CVPR*, pages 1024–1033, 2018. [2](#)
- [48] Hongzu Su, Jingjing Li, Zhi Chen, Lei Zhu, and Ke Lu. Distinguishing unseen from seen for generalized zero-shot learning. In *CVPR*, pages 7875–7884, 2022. [2](#)
- [49] Laurens van der Maaten and Geoffrey Hinton. Visualizing data using t-sne. *Journal of Machine Learning Research*, 9:2579–2605, 2008. [7](#)
- [50] Vinay Kumar Verma, Gundeep Arora, Ashish Mishra, and Piyush Rai. Generalized zero-shot learning via synthesized examples. In *CVPR*, pages 4281–4289, 2018. [2](#)
- [51] Maunil R Vyas, Hemanth Venkateswara, and Sethuraman Panchanathan. Leveraging seen and unseen semantic relationships for generative zero-shot learning. In *ECCV*, pages 70–86, 2020. [6](#)
- [52] Catherine Wah, Steve Branson, Peter Welinder, Pietro Perona, and Serge J. Belongie. The caltech-ucsd birds-200-2011 dataset. 2011. [5](#)
- [53] Chaoqun Wang, Shaobo Min, Xuejin Chen, Xiaoyan Sun, and Houqiang Li. Dual progressive prototype network for generalized zero-shot learning. In *NeurIPS*, pages 2936–2948, 2021. [2](#), [6](#)
- [54] Henan Wang, Muli Yang, Kun Wei, and Cheng Deng. Hierarchical prompt learning for compositional zero-shot recognition. In *IJCAI*, page 3, 2023. [2](#)
- [55] Xiaolong Wang, Yufei Ye, and Abhinav Gupta. Zero-shot recognition via semantic embeddings and knowledge graphs. In *CVPR*, pages 6857–6866, 2018. [1](#)
- [56] Zifeng Wang, Zizhao Zhang, Sayna Ebrahimi, Ruoxi Sun, Han Zhang, Chen-Yu Lee, Xiaoqi Ren, Guolong Su, Vincent Perot, Jennifer Dy, et al. Dualprompt: Complementary prompting for rehearsal-free continual learning. In *ECCV*, pages 631–648, 2022. [2](#)
- [57] Zifeng Wang, Zizhao Zhang, Chen-Yu Lee, Han Zhang, Ruoxi Sun, Xiaoqi Ren, Guolong Su, Vincent Perot, Jennifer Dy, and Tomas Pfister. Learning to prompt for continual learning. In *CVPR*, pages 139–149, 2022. [2](#)
- [58] Jiamin Wu, Tianzhu Zhang, Zheng-Jun Zha, Jiebo Luo, Yongdong Zhang, and Feng Wu. Prototype-augmented self-supervised generative network for generalized zero-shot learning. *TIP*, 33:1938–1951, 2024. [2](#)
- [59] Yongqin Xian, Zeynep Akata, Gaurav Sharma, Quynh Nguyen, Matthias Hein, and Bernt Schiele. Latent embeddings for zero-shot classification. In *CVPR*, pages 69–77, 2016. [2](#)
- [60] Yongqin Xian, Christoph H Lampert, Bernt Schiele, and Zeynep Akata. Zero-shot learning—a comprehensive evaluation of the good, the bad and the ugly. *TPAMI*, 41:2251–2265, 2018. [5](#)
- [61] Yongqin Xian, Tobias Lorenz, Bernt Schiele, and Zeynep Akata. Feature generating networks for zero-shot learning. In *CVPR*, pages 5542–5551, 2018. [2](#)
- [62] Guo-Sen Xie, Li Liu, Xiaobo Jin, Fan Zhu, Zheng Zhang, Jie Qin, Yazhou Yao, and Ling Shao. Attentive region embedding network for zero-shot learning. In *CVPR*, pages 9384–9393, 2019. [1](#), [2](#)
- [63] Wenjia Xu, Yongqin Xian, Jiuniu Wang, Bernt Schiele, and Zeynep Akata. Attribute prototype network for zero-shot learning. In *NeurIPS*, 2020. [1](#), [2](#), [6](#)
- [64] Dongran Yu, Xueyan Liu, and Bo Yang. Zero-shot image classification with logic adapter and rule prompt. In *ACM*, pages 2075–2084, 2024. [6](#)

- [65] Li Zhang, Tao Xiang, and Shaogang Gong. Learning a deep embedding model for zero-shot learning. In *CVPR*, pages 3010–3019, 2017. [1](#), [2](#)
- [66] Xun Zhang, Yang Liu, Yuhao Dang, Xinbo Gao, Jungong Han, and Ling Shao. Adaptive relation-aware network for zero-shot classification. *Neural Networks*, 174:106227, 2024. [2](#)
- [67] Peng Zhao, Qiangchang Wang, and Yilong Yin. M3r: Masked token mixup and cross-modal reconstruction for zero-shot learning. In *ACM*, pages 3161–3171, 2023. [1](#)
- [68] Yuan Zhou, Lei Xiang, Fan Liu, Haoran Duan, and Yang Long. Dynamic visual-guided selection for zero-shot learning. *J. Supercomput.*, 80:4401–4419, 2024. [2](#)
- [69] Yizhe Zhu, Jianwen Xie, Zhiqiang Tang, Xi Peng, and Ahmed Elgammal. Semantic-guided multi-attention localization for zero-shot learning. In *NeurIPS*, pages 14917–14927, 2019. [1](#)